Net phytoplankton discriminating patches along the southern Black Sea coast in winter 1990

Southern Black Sea
Net phytoplankton
Winter productivity
Multi-Dimensional Scaling

Mer Noire méridionale
Phytoplancton
Productivité hivernale
Échelle multi-dimensionnelle

Zahit UYSAL and Halil İ. SUR

Institute of Marine Sciences, Middle East Technical University, P.B. 28, 33731, Erdemli-Içel, Turkey.

Received 13/12/94, in revised form 07/09/95, accepted 12/09/95.

ABSTRACT

Cold water formed on the western continental shelf of the Black Sea in February 1990 was studied. The band of cold water follows the coast and interacts with coastal geometry, resulting in winter phytoplankton blooms particularly along the southwestern coast. Species composition and surface spatial distribution of net phytoplankton (> 55 μm) showed an apparent species differentiation between the shelf and open ocean plankton. Offshore waters exhibit high diversity indices compared to shelf waters where the intense outburst induced by *Chaetoceros* sp. occurs. This species of diatom thrived successfully in the cold waters, reaching cell densities > 10^6 cells/l in the vicinity of Sakarya river and its eastward extension.
Six different-sized patchy aggregates were determined along the coast by using multivariate analysis (cluster and Multi-Dimensional Scaling, MDS) technique.

RÉSUMÉ

Les peuplements phytoplanctoniques le long de la côte méridionale de la mer Noire pendant l'hiver 1990.

Une veine d'eau froide a été observée au cours de l'hiver 1990 sur le plateau continental du bassin oriental de la mer Noire. Cette veine, qui s'écoule vers l'est le long de la côte en formant des méandres liés à la topographie côtière, est le siège de floraisons phytoplanctoniques surtout localisées sur le bord sud-ouest. La répartition spatiale ainsi que la composition des peuplements phytoplanctoniques (> 55 μm) montrent des différences nettes entre les eaux côtières et celles du large. L'indice de diversité est beaucoup plus élevé au large que dans les zones néritiques où les eaux froides favorisent le développement de diatomées du genre *Chaetoceros* dont les populations atteignent des densités cellulaires supérieures à 10^6 cellules/litre. Une analyse multivariée permet de distinguer six zones majeures de concentrations phytoplanctoniques de différentes ampleurs.

Oceanologica Acta, 1995, **18**, 6, 639-647.

INTRODUCTION

The upper ocean circulation derived from hydrographic measurements (the so-called Rim Current, Oğuz *et al.*, 1993, 1994) is described by a well defined cyclonic boundary current approximately following the narrow continental slope region, and a series of semi-permanent anticyclonic eddies on the periphery between the boundary current and the undulations of the coast (Fig. 1). The meandering nature of the boundary current is possibly responsible for these standing structures as well as transient features along the periphery. The strong boundary current limits the water and material transfer across the flow, while jet instabilities, mesoscale eddies, filaments, mushroom-like structures and similar phenomena play important roles in the cross-shelf exchanges.

The northwestern shelf and the Bosphorus vicinity are the two major areas where lateral sources and convection modify the Black Sea circulation. The competing effects of

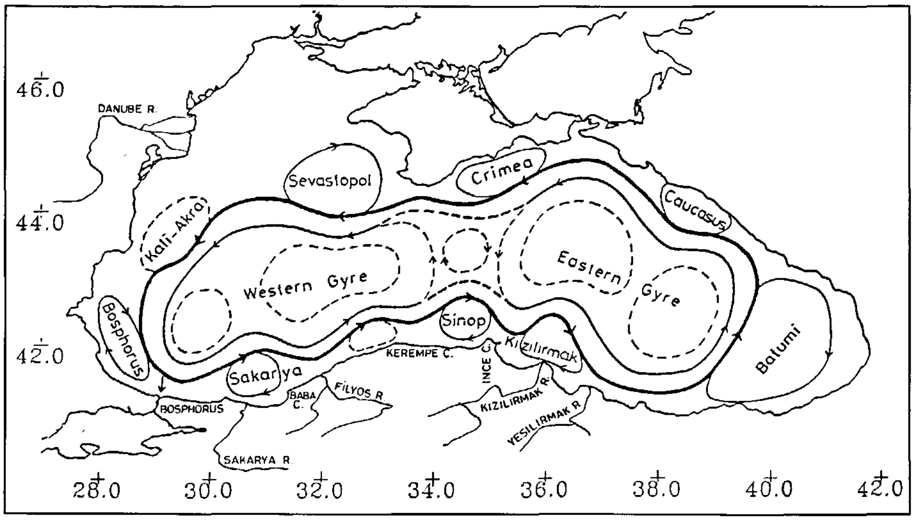

Figure 1

Schematized general circulation of the Black Sea (after Oguz et al., *1993).*

freshwater inflow and winter cooling respectively create and destroy vorticity in the first area (Stanev, 1990), while intermediate depth intrusion driven by shelf mixing of the dense Mediterranean inflow creates similar disturbances in the second area (Stanev, 1990; Özsoy *et al.*, 1993).

Salinity observations near the Anatolian coast suggest that the fresh water from the northwest shelf reaches the southwest coast. Sur *et al.* (1994) computed the mean salinity of the surface waters within the upper 10 m in the southwestern Black Sea (between 28 and 32° E, and 41 and 42° N) from long-term CTD data. The weight of the data indicates a mean salinity of about 18 in the southwest sector of the Black Sea, decreasing to 16-17 when the Danubian influence is felt the area.

The Black Sea is known to be a region of moderate to high productivity since it is fed by a rich supply of nutrients in comparison with other parts of the world ocean (Koblentz-Mishke *et al.*, 1970). Sorokin (1983) indicated that peaks in the primary productivity of the Black Sea were known to occur twice a year, with a major bloom principally composed of diatoms in early spring, followed by a secondary bloom mainly comprising coccolithophorids in autumn. Occasional blooms of coccolithophorids and dinoflagellates occurred, mainly in coastal areas. Additional summer blooms with a predominance of dinoflagellates and coccolithophorids (*Emiliana huxleyi*) have been increasingly observed in the region in recent years (Bologa, 1986; Benli, 1987; Hay *et al.*, 1989, 1990, 1991). Sorokin (1983) also reported the spring and summer development of red tides in the western shelf region. Massive red tides have been created along the Romanian and Bulgarian coasts by dinoflagellates (Sukhanova *et al.*, 1988). There are limited observations for the winter season; one of them, indicating massive blooms of certain plankton species along the western Anatolian coast, is the subject of the present work.

The maximum spring-autumn primary productivity (60 % of the Black Sea production) is found on the northwest shelf, where 87 % of the total fresh water input enters the Black Sea from major rivers, contributing large amounts of nutrients and detritus to the shallow shelf region and reducing surface salinity and transparency. The next highest primary productivity is reported to occur along the Romanian (western) and the Anatolian (southwestern) coasts, and extends into the central region that separates the eastern and western gyres (Bologa, 1986). This limited observation suggests that the western Anatolian coast is also a region of relatively high productivity. Open-sea primary productivity at the centres of the western and eastern gyres of the Black Sea is typically low.

In order to obtain a better understanding of the scale-dependent spatial pattern of the net phytoplankton community in relation to prevailing surface current regime along the Anatolian coast of the Black Sea, this study was performed at 139 stations within the Turkish EEZ (Exclusive Economic Zone) in February 1990.

MATERIAL AND METHODS

In the area extending from approximately 28° E to 41° E, near-surface (≈5 m) plankton data were collected with 5-litre closing bottles. Total volumes of 5 to 15 litres, depending on the phytoplankton density, were filtered on board through a mesh size net 55-micrometre; filters were preserved in a borax-buffered 4 % seawater-formalin solution. For the counting of phytoplankters, aliquots of 0.1 ml from the concentrates were examined over a Palmer-Maloney chamber under the microscope. Each counting involved as far as possible at least 400 cells (Venrick, 1978). Acid washing of the samples was done according to the method described in Baltic Sea Environment Proceedings (1988) for the qualitative analysis of diatoms. In this method, *ca.* 1 ml conc. HNO_3 is added to 0.5 ml of concentrated sample and the sample tube heated on a small flame under the fume hood. After boiling for 1-5 minutes until the solution is relatively clear, white vapours start to form. If the material is not completely oxidized after five minutes, a few drops of concentrated H_2SO_4 are added and kept over the heat. The sample is then transferred to a centrifuge tube filled with *ca.* 10 ml distilled water, and centrifuged at 1500 rpm for 20 minutes. After drainage of the supernatant water, the same procedure is repeated at least five times.

A total of 139 stations were surveyed with the Turkish research vessel R/V *Bilim* of the Institute of Marine Sciences-Middle East Technical University (IMS-METU). During this cruise (8-28 February 1990), CTD measurements were performed at 70 hydrographic stations. The 139 stations were grouped into 23 grids, taking the mean values of the abundance of each species in each grid for the analysis of multispecies data via multivariate techniques – Multi-Dimensional Scaling. Grouping the 139 stations this fashion also eliminates likely computational problems for large numbers of stations, as the computer time increases proportionally to n and tends to become prohibitive for 3-figure values of n. Stations positioned on the longitudinal lines are included in the grids to the right as the boundary current flows eastwards.

Images produced by the AVHRR (Advanced Very High Resolution Radiometer) sensor of NOAA satellites and CTD measurements were used to reflect the flow characteristics of the Black Sea boundary current system. Image processing was done on the SEAPAK interactive processing system at the IMS-METU.

Analytical Methods

For the analysis of survey data, biotically similar samples are grouped for statistical differences, avoiding the influence of any previous assumptions about relationships between the biota and the environment. Analysis of multispecies data was done utilizing both STATGRAPHICS (Univariate Statistics Package) and PRIMER (Multivariate Analyses Package – Plymouth Routines in Multivariate Ecological Research), PC programs written at the Plymouth Marine Laboratory. The multivariate statistical technique was preferred, since it determines which environmental factors have the greatest influence in determining species distributions and the degree of confidence with which one can infer these variables from diatom species composition.

The data set required root-root (4^{th} root) transformation to adjust the weight of abundant species. Its advantage in comparison with logarithmic transformation is that, when similarity is assessed by the Bray-Curtis measure, the similarity coefficient is invariant to a scale change, *e.g.* scores may be expressed as per cm^2 or per m^2.

$$Y_{ij} = \sqrt{\sqrt{X_{ij}}} = X_{ij}^{1/4}$$

where X = raw data score of the i^{th} species in the j^{th} sample,
Y = corresponding transformed score

In order to assess similarity, the BRAY-CURTIS Coefficient – one of the most common methods in ecological studies – is used.

Similarity between j^{th} and k^{th} samples is:

$$S_{jk} = 100 \{1 - \textstyle\sum_i |y_{ij} - y_{ik}| \;/\; \textstyle\sum_i (y_{ij} + y_{ik})\}$$

where y_{ij} = score (count) for i^{th} species in j^{th} sample,
y_{ik} = score for the i^{th} species in the k^{th} sample.

Then the similarity matrix is formed between every pair of pooled samples (grids) in a lower triangular array for further clustering and ordination. Application of the measure of similarity results in a triangular matrix whose entries compare each of (n) samples with every other sample. For a graphic representation of relations among sites, a dendogram showing clustered groups at an arbitrary cut-off level of 50 % was constructed. Among the various hierarchical sorting strategies, group-average sorting is preferred for the production of a dendogram from the similarity matrix, as it joins two groups of samples together at the average level of similarity between all members of one group and all members of the other. In order to visualize sample (site) relationships, ordination was done by delineating dendogram classes on the corresponding ordination via Multi-Dimensional Scaling (MDS).

The contribution to average dissimilarity ($\bar{\delta}$) or similarity ($\bar{S}$) from i^{th} species is calculated to determine the discriminating species responsible for groupings among the community.

Simply δ = 100-S, and the contribution to δ_{jk} from i^{th} species is:

$$\delta_{jk}(i) = 100\,|y_{ij} - y_{ik}| \;/\; \textstyle\sum_i (y_{ij} + y_{ik})$$

δ_{jk} then averaged over all pairs (with j in 1^{st} and k in 2^{nd} group) to give average contribution $\bar{\delta}_i$ from i^{th} species. Its standard deviation is given as $SD(\delta_i)$ in the context.

High $\bar{\delta}_i$ and a high ratio of $\bar{\delta}_i/SD(\delta_i)$ singled out the discriminating species. Further, the contribution of the i^{th} species ($\bar{\delta}_i$) to the average similarity within a group ($\bar{S}$) was similarly computed. This indicates that the species concerned is consistently prominent in that group (Anon., 1992).

Species richness is often given simply as the total number of species (S), which is obviously highly dependent on sample size, but more commonly as MARGALEF's INDEX d, which also incorporates the total number of individuals (N);

$$d = (S - 1) / \ln N$$

where S = the number of species,
N = the number of individuals.

In addition to this, the SHANNON-WIENER (Anon., 1992) INDEX – which is the most commonly used diversity measure – is calculated. This index incorporates both the species richness and equitability components.

$$H' = -\textstyle\sum_i P_i (\ln P_i)$$

where P_i is the proportion of the i^{th} species of the whole sample.

For a measure of proportional representation (Equitability) PIELOU's EVENNESS INDEX (Anon., 1992) is used to express the degree of evenness in the distribution of individuals among different species,

$$J = H'(\text{observed}) / H'_{max}$$

where H'_{max} is the maximum possible diversity (ln S).

Calculations for species richness and diversity measures are based on the previously grouped 23 grids.

RESULTS

Analysis of *in situ* and satellite data

The only available cloud-free infrared (AVHRR) image on 27 February, 1990 (Fig. 2*a*) indicates cold water with uniform temperatures along the entire western continental shelf. This well-mixed water has a uniform temperature of ≈ 6.5 °C and salinity of less than 18 in the upper 30-40 m along the southern coast (Fig. 2*b, c*). The boundary of the cold water follows a constant depth contour between 50 and 100 m along the entire western shelf. The width of this band of cold water decreases towards the south, parallel to the decreasing width of the shelf. It then becomes so thin that it is hardly noticeable along the southwestern shelf. Since it is so thin, the cold water hugs the coast and is transported along the shallow inner part (<100 m) of the Sakarya Canyon without creating any disturbance there (Fig. 2*a*). When the rim current transporting the cold water reaches the concave coastline east of the Canyon, it flows north and expands near Cape Baba where the narrow shelf topography is terminated. The temperature structure displayed in Figures 2*a, b* near this Cape is very similar to a shock; the narrow band of cold water suddenly expands and continues to flow along the coast with a sudden increase in width.

The dynamic topography in Figure 2*d* displays boundary currents with alongshore variations. The current becomes discontinuous near the Bosphorus. This region of discontinuous currents could indicate a coastal attachment of the current (Fig. 2*a, c*) not sufficiently resolved by the geostrophic analyses. It should be noted that the width of the boundary current increases downstream of Sakarya Canyon. This implies a shock, or a critical transition, which may be associated with the effects of Cape Baba. The cold water separation from the coast in Figure 2*b* occurs at the same location where the streamlines indicate a surface divergence in Figure 2*d*.

A reference level of 300 dbar was used in dynamic computations. The dynamic height is calculated in cm units, and the observational mean is subtracted. The objective analyses are made on a regular grid of (1/4)° spacing, using a correlation model fitted to the observations.

In Figure 2*a*, we also identify warm water along the continental slope offshore of the shelf waters, which gradually disappears by frontal mixing with the cold shelf water on the western and southern coasts. This gradual admixture of the cold and warm waters proceeds along the coast from the northwest shelf to the vicinity of Cape Baba. The tongue of cold water diminishes towards the east after its separation from the coast as far as Cape Ince, as is evident in Figure 2*b*.

Species Diversity Indices

The three-week cruise along the Turkish coast in February 1990 revealed that the majority (≈ 60 %) of the total 120 species encountered comprised Bacillariophyta (Diatom). Dinoflagellates formed the second major group (≈ 34 %) and the remainder belonged to other phyla. From the taxonomic point of view, an increase in the dinoflagellate percentage ratio (from 16 % to 34 %) is evident when compared to the ratios given for the Black Sea by Bologa (1986). This is also true for the April 1990 cruise, which yielded almost the same ratios of diatoms to dinoflagellates (Uysal, 1993). Another unique feature was the invasion of a centric diatom *Chaetoceros* sp. in the band of cold water attached to the shore on the west Anatolian Black Sea coast. This sole species of *Chaetoceros* sp. could not be identified to a species level due to its loose frustule which also disfavoured acid washing. Species percentage frequency distribution clearly showed that *Chaetoceros* sp. accounted for ≈ 90 % of all species, and was followed by *Skeletonema costatum* (≈ 6 %). Both species have also been reported from the Romanian Black Sea coast as the dominant winter species (Bologa *et al.*, 1984).

The total number of species identified in the western part greatly exceeded the number encountered in the east. As may be clearly seen from Figures 3 and 4, the west coast, especially the alternating coastal grid stations 1, 3, 4, 5, 6, 7, 8, and 9, all of which extend within the band of cold water (Fig. 2*a, b*) flowing eastwards along the western Anatolian coast, proved to be the most productive region. Two of them (grids #4 and #5), corresponding to the Sakarya river effluent and its eastern extension, exceeded 10^6 cells/l. Similarly, this sector also reached a maximum cell density in April 1989 (Uysal, 1993). To the east of Sakarya Canyon, phytoplankters flowered abundantly in the coastal region near Cape Baba, gridded as #5. Diatom species of *Chaetoceros* sp. and *Chaetoceros diadema* dominated the bloom in this region.

Species differentiation in the shelf and offshore water plankton is apparent, with offshore waters remaining at relatively low species levels in comparison with the species-rich south-western Black Sea shelf waters between the Bosphorus junction of the Black Sea and Cape Ince (Tab. 1).

Table 1

Variation in phytoplankton community diversity indices at the surface along the Turkish Black Sea coast in February 1990.

Grid #	Total cell abundance	Total # species	Richness d	Shannon H'	Evenness J'
1	585081	22	1.58	0.06	0.02
2	131	7	1.23	1.32	0.68
3	143683	39	3.20	0.59	0.16
4	1141026	53	3.73	0.09	0.02
5	1626292	51	3.50	0.09	0.02
6	912097	54	3.86	0.07	0.02
7	435	15	2.30	1.64	0.61
8	579517	42	3.09	0.14	0.04
9	226528	42	3.33	0.43	0.11
10	67933	38	3.33	0.97	0.27
11	10945	22	2.26	1.10	0.36
12	6764	26	2.84	1.29	0.40
13	191204	32	2.55	0.29	0.08
14	3154	15	1.74	0.82	0.30
15	3886	19	2.18	1.39	0.47
16	25654	22	2.07	0.56	0.18
17	97512	22	1.83	0.28	0.09
18	719	20	2.89	1.68	0.56
19	1166	8	0.99	0.95	0.46
20	297	9	1.41	1.44	0.66
21	736	19	2.73	1.18	0.40
22	737	24	3.48	2.12	0.67
23	1761	21	2.68	1.54	0.51

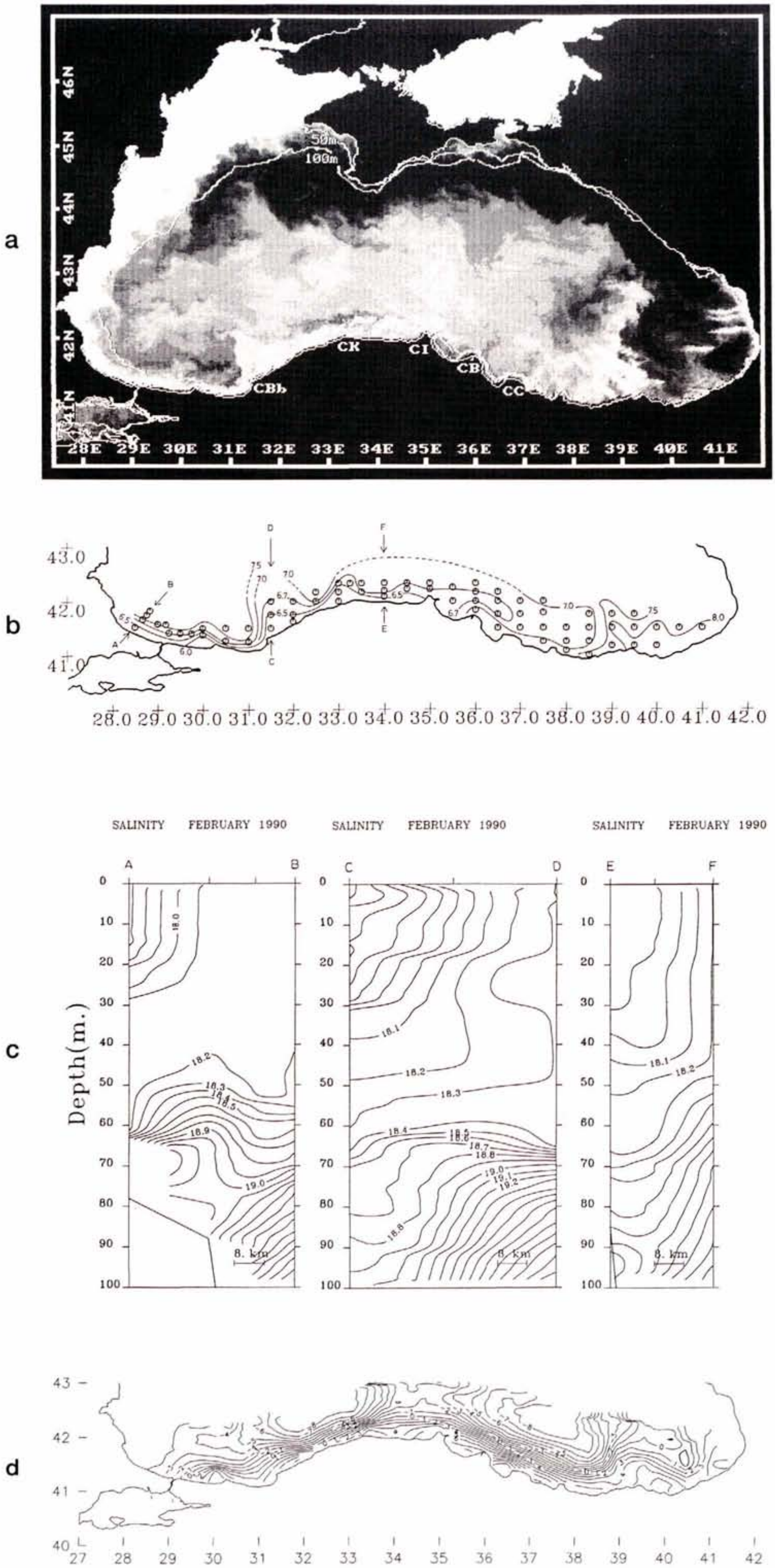

Figure 2

(a) *Advanced Very High Resolution Radiometer (AVHRR) satellite image on 27 February, 1990 (NOAA-10 Channel 4, Lighter tones represent the colder waters, Abbreviations used; CBb:Cape Baba, CK: Cape Kerempe, CI: Cape Ince, CB: Cape Bafra),* (b) *Surface temperature distribution and* (c) *cross-shore hydrographic sections depicted by arrows in* (a), *during the February 1990 cruise of R/V* Bilim, (d) *Surface dynamic topography (cm), referenced to 300 m during the February 1990 cruise of the R/V* Bilim.

As stated by Malone (1980), the net plankton fraction increases in relative abundance in continental shelf waters where chain-forming diatoms and large solitary diatoms and dinoflagellates dominate the phytoplankton. Species richness was higher between the Sakarya and Filyos rivers and reached its maximum (d = 3.86) around Cape Baba where the narrow band of cold flow suddenly widens.

Off the Bosphorus entrance at grid #2, where the warmer waters of the continental slope prevail, observed species number and density were lowest (Fig. 3, Tab. 1). As the offshore limits (upper sections) of grids #1 and #7 mix with the open warmer waters, a sharp decrease in density and species richness was observed in comparison to coastal grids influenced almost entirely by the cold water, as displayed in Figure 2. The westernmost grid #1 holds three times as many species as grid #2 and is richer in abundance (Tab. 1), implying that its lower section is partly influenced by the coastally attached cold flow. It is important to note here that the satellite image describes the situation at the end of February, and that plankton sampling ended the following day. It is thus rather difficult to delimit such temporary features when patches are considered within a lenghty time span. The degree of mixing of warmer water plankton with those which thrive in colder waters will be discussed below, with reference to a two-dimensional non-metric (MDS) ordination of grid stations along the coast.

The density of species along the eastern part of the Anatolian coast remained very low, with the exception of somewhat higher levels in front of Yesilirmak river and its eastern component (Fig. 4, Tab. 1). The intense flowering of the neritic species *Skeletonema costatum* and –to a lesser extent– *Nitzschia longissima* around Yesilirmak was responsible for a local enrichment in cell abundance. In areas where a single species dominated the community, the lowest equitability measures (J′) are observed (Tab. 1). Such weakness in proportional representation (J′) is characteristic of the most productive regions around Sakarya and Filyos rivers in the western part, and Yesilirmak in the eastern part.

Significant features of the blooming sites were lower proportional representation (J′) among the species and diversity (H′), due to intense flowering of a single species (*Chaetoceros* sp.), especially in the western sector (Tab. 1). In contrast, the diversity and proportional representation of species were much higher in the east. Species richness (d) in the western part was higher due to larger patch size rich in both abundance and species. More than 50 species have been identified between the Sakarya and Filyos rivers.

Multi-Dimensional Scaling

Figure 5 shows two-dimensional non-metric MDS plots of gridded surface stations having six distinct groups at an arbitrary similarity level of 50 % (Fig. 6). It may be clearly seen that plankton sampled from warmer water (group III,

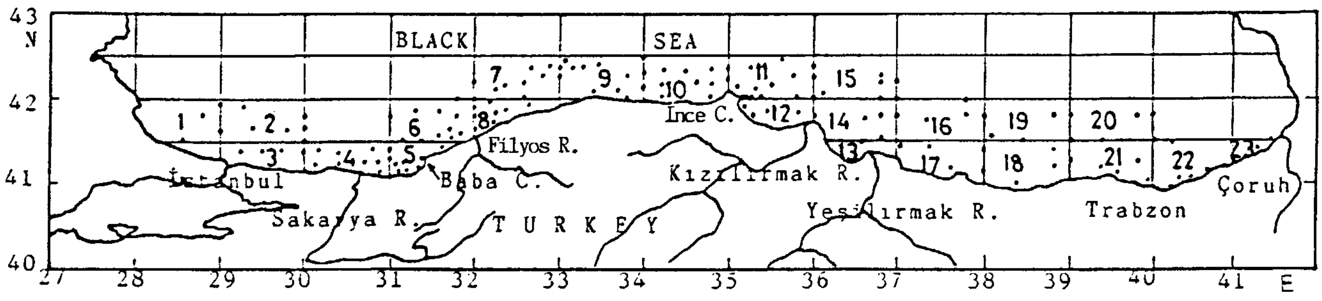

Figure 3

Sampling stations and locations of grid stations along the Turkish coast.

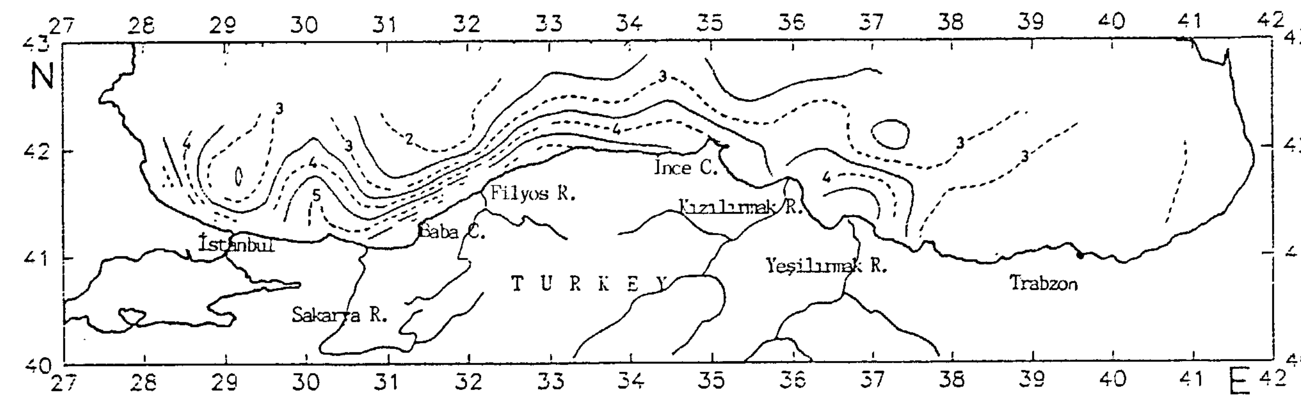

Figure 4

Surface spatial distribution of net phytoplankton abundance along the coast in February 1990 (log_{10}[cells/l]).

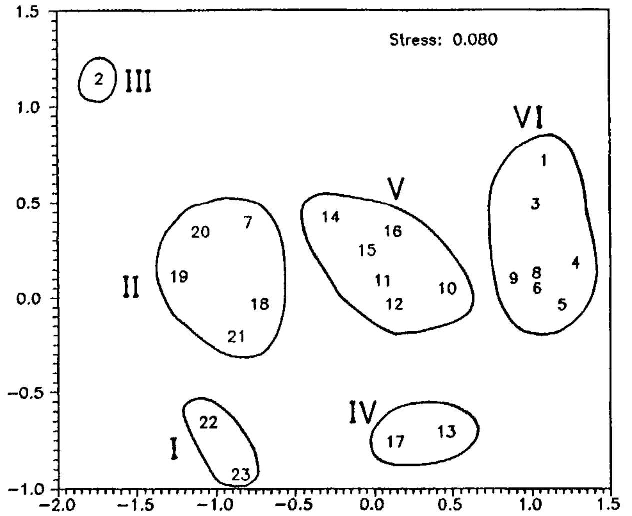

Figure 5

Two-dimensional non-metric MDS (Multi-Dimensional Scaling) ordination of the 23 grid stations.

grid #2) is separated from the remainder with its lowest abundance and species richness located off the Bosphorus. The neighbouring grids #1 and #3, partly sharing the colder water species possibly carried by the boundary current from the northwest shelf, are placed within the larger most productive group (VI). Subgrid stations 1, 3, 4, 5, 6, 8 and 9, all placed on the route of cold water shown in Figure 2, form a large group (VI) which is distinguished from the others by higher abundance and species richness. Grid #7, bearing mostly the offshore warmer water species, and characterized by low abundance, does not appear within this rich group. Only 15 species have been encountered, whereas the mean of group VI is 43 species.

It is interesting to note that grid #7, together with the most easterly grids #18, #19, #20, and #21 constitutes another group (II). Surface temperature contours (Fig. 2*b*) of the same cruise along the coast reveal that relatively warmer (7 °C) offshore waters coexist in both sectors extending up to 39° E. Group II is clearly separated from the central group V. Group IV, directly influenced by the Yesilirmak river, was rich in cell density. Higher phytoplankton abundance around Yesilirmak to the east (Grids #13, #16, and #17) implies enrichment *via* river input. However, this was not true for the Kizilirmak river. The effect of temperature on groupings is also apparent in the much warmer easternmost sector. Two of the easternmost coastal grids, #22 and #23, both exhibited more species and higher diversity, distinguishing them from the adjacent community.

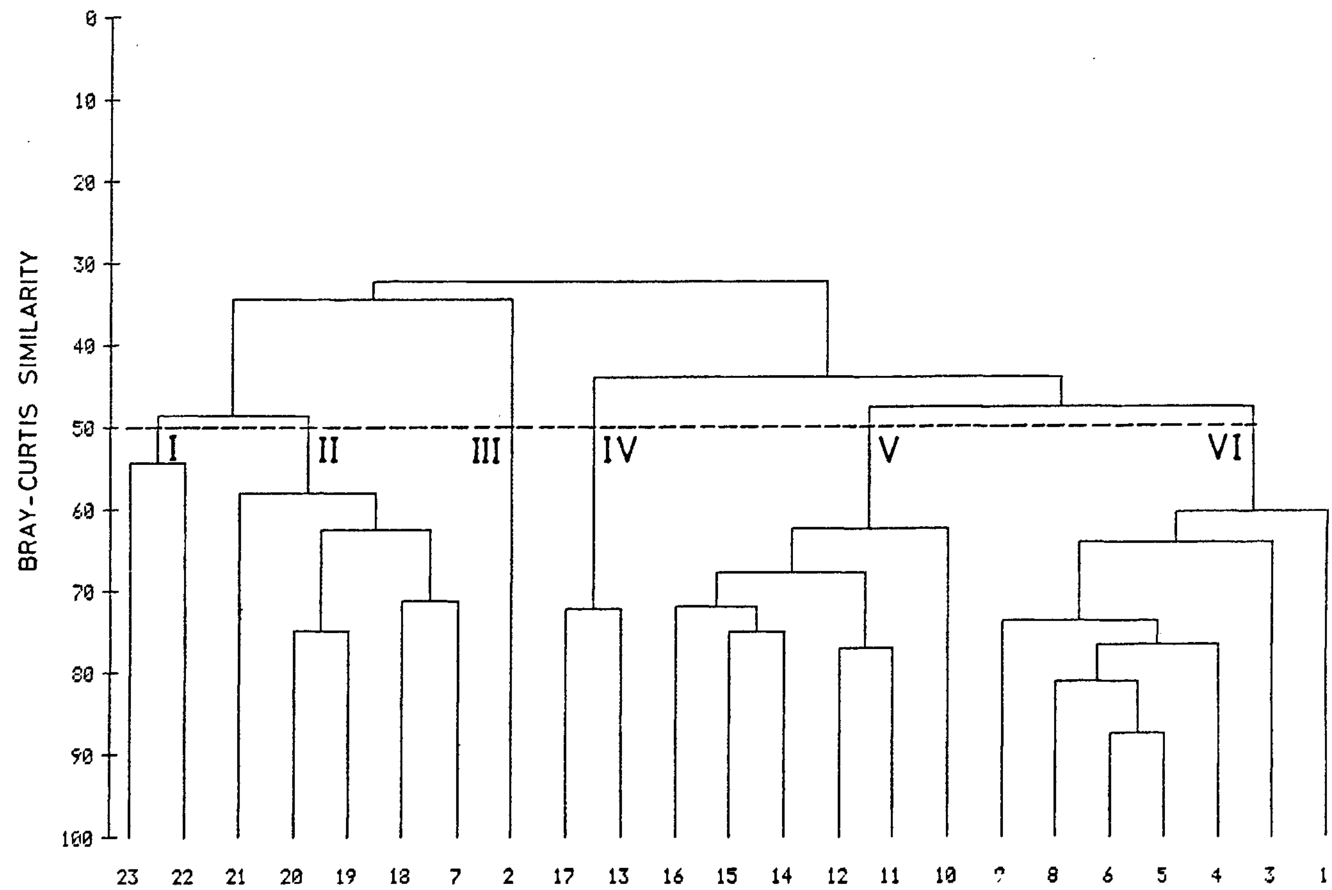

Figure 6

Dendogram showing classification of the 23 grid stations with six major groups distinguished at an arbitrary similarity level of 50 %.

Table 2

Species contribution ($\bar{S}_i$) to average similarities ($\bar{S}$) within groups. Groups I, III and IV are not included, due to low similarity values.

Group	Species	$\bar{S}_i$	SD(S_i)	$\bar{S}_i$/SD(S_i)	$\sum\bar{S}_i$ %
*62.8	*Fragilaria capucina*	12.8	3.2	4.0	20.4
	Chaetoceros sp.	11.0	1.6	6.8	37.9
II	*Nitzschia longissima*	10.8	2.0	5.3	55.1
	Skeletonema costatum	9.1	1.6	5.7	69.6
	Coscinodiscus sp.	4.4	1.4	3.3	76.6
*67.6	*Leptocylindrus minimus*	12.0	2.4	5.1	17.7
	Nitzschia longissima	10.1	1.8	5.6	32.7
V	*Chaetoceros* sp.	9.4	3.8	2.5	46.6
	Fragilaria capucina	4.7	0.8	6.1	53.5
	Peridinium pellucidum	3.8	0.6	7.0	59.2
*69.3	*Chaetoceros* sp.	19.3	3.7	5.2	27.8
	Chaetoceros diadema	4.9	1.0	4.8	34.9
VI	*Nitzschia longissima*	4.2	1.3	3.3	40.9
	Peridinium pellucidum	3.3	0.5	6.4	45.7
	Coscinodiscus sp.	3.0	0.3	8.9	50.0

* Average similarity ($\bar{S}$) within the group.

Table 3

Species contribution ($\bar{\delta}_i$) to total average dissimilarity. ($\bar{\delta} = \sum\bar{\delta}_i$) between groups.

Group	Species	$\bar{\delta}_i$	SD(δ_i)	$\bar{\delta}_i$/SD(δ_i)	$\sum\bar{\delta}_i$ %
*51.4	*Diatoma vulgare*	3.2	1.8	1.8	6.1
	Navicula radiosa	3.0	1.4	2.1	11.9
II&I	*Ceratoneis arcus*	2.5	1.6	1.6	16.7
*78.3	*Chaetoceros* sp.	6.9	1.3	5.3	8.8
	Diatoma vulgare	5.9	0.4	14.8	16.2
III&I	*Actinastrum hantzschii*	5.1	0.1	51.0	22.7
*60.6	*Chaetoceros* sp.	8.0	1.3	6.2	13.3
	Actinastrum hantzschii	7.6	1.5	5.1	25.7
III&II	*Fragilaria capucina*	3.9	3.2	1.2	32.2
*65.2	*Skeletonema costatum*	13.9	0.8	17.4	21.4
	Nitzschia longissima	4.2	0.8	5.3	27.8
IV&I	*Nitzschia delicatissima*	3.1	0.3	10.3	32.6
*62.4	*Skeletonema costatum*	16.2	1.4	11.6	25.9
	Nitzschia longissima	6.3	1.3	4.8	36.1
IV&II	*Nitzschia delicatissima*	3.5	0.6	5.8	41.7
*82.3	*Skeletonema costatum*	20.3	1.9	10.7	24.6
	Nitzschia longissima	8.6	0.8	10.8	35.0
IV&III	*Nitzschia delicatissima*	4.3	0.3	14.3	40.2
*64.1	*Leptocylindrus minimus*	7.6	1.1	6.9	11.9
	Chaetoceros sp.	4.4	2.9	1.5	18.8
V&I	*Diatoma vulgare*	3.1	1.1	2.8	23.7
*54.0	*Leptocylindrus minimus*	8.9	2.0	4.5	16.5
	Chaetoceros sp.	6.0	3.8	1.6	27.6
V&II	*Nitzschia longissima*	4.0	2.2	1.8	35.0
*74.4	*Chaetoceros* sp.	11.2	4.5	2.5	15.1
	Leptocylindrus minimus	11.2	2.0	5.6	30.2
V&III	*Nitzschia longissima*	6.4	2.0	3.2	38.8
*54.1	*Skeletonema costatum*	13.0	1.7	7.6	24.0
	Leptocylindrus minimus	5.8	1.1	5.3	34.7
V&IV	*Chaetoceros* sp.	4.1	2.8	1.5	42.2
*76.0	*Chaetoceros* sp.	14.2	3.0	4.7	18.7
	Chaetoceros diadema	4.3	0.8	5.4	24.3
VI&I	*Ditylum brightwellii*	3.0	1.8	1.7	28.2
*74.0	*Chaetoceros* sp.	16.4	3.5	4.7	22.2
	Chaetoceros diadema	4.6	1.1	4.2	28.4
VI&II	*Ditylum brightwellii*	3.3	2.1	1.6	32.9
*87.1	*Chaetoceros* sp.	0.3	4.3	4.7	23.3
	Chaetoceros diadema	.3	1.0	5.3	29.4
VI&III	*Ditylum brightwellii*	.7	2.5	1.5	33.6
*58.0	*Chaetoceros* sp.	12.5	2.9	4.3	21.6
	Skeletonema costatum	7.4	1.9	3.9	34.4
VI&IV	*Chaetoceros diadema*	3.6	0.8	4.5	40.7
*52.4	*Chaetoceros* sp.	11.1	4.1	2.7	21.2
	Chaetoceros diadema	3.0	1.3	2.3	26.9
VI&V	*Ditylum brightwellii*	2.6	1.8	1.4	31.9

* Average dissimilarity ($\bar{\delta}$) between the groups.

The Bray-Curtis similarity matrix has shown that highest similarity is observed between grids along the west coast where blooming took place (Fig. 6). Among all the 23 grid stations, the degree of sharing of the same species with the remainder was lowest with grid #2. However, species clustering or ordination is generally less informative than methods which highlight species that contribute to patterns of sample clustering or ordination. Discriminating species for the sites and within the groups responsible for such patchy distribution are tabulated in Tables 2 and 3. Six groups as displayed in Figures 5 and 6 are worked out to determine the major discriminating species of such clusters.

Higher species contribution ($\bar{S}_i$) and ratio {$\bar{S}_i$/SD(S_i)} highlight species consistently prominent in a given group. Table 2 indicates that *Chaetoceros* sp, *C. diadema* and *Nitzschia longissima*, with higher ratios, contributed much to the similarity in group VI. Similarly, two of these species, *Chaetoceros* sp. and *Nitzschia longissima*, also contributed much to the central group (V). In the eastern group (II), *Fragilaria capucina*, *Chaetoceros* sp. and *Nitzschia longissima* were consistently prominent.

Species discriminating groups are given in Table 3. In the west, group III separated from the nearby group VI lacking diatom species of *Chaetoceros* sp, *Chaetoceros diadema* and *Ditylum brightwellii*. These species also played a major role in distinguishing the productive western group from the other eastern groups. It is apparent that the dominant species *Chaetoceros* sp. played a significant role in such distinction among patches formed along the Turkish Black Sea coast.

CONCLUSIONS

In February 1990, a thin band of cold water flows along the shallow southwestern shelf; then, following the inner part of Sakarya Canyon, it becomes separated from the coast and takes the form of a shock at Cape Baba, where the narrow shelf topography is terminated. It is evident that the advection of cold, well-mixed water along the shelf regions of the western Black Sea has an important impact on winter net phytoplankton distribution.

A phytoplankton count carried out along the Turkish coast during this month indicated an intense bloom along the coast, first following the vein of cold water to Cape Baba, and then occurring in the separated flow region up to Cape Kerempe, in the same area where cold water was observed in the satellite image. Diatom *Chaetoceros* sp. was dominant throughout the survey area, having an abundance of more than 91 % with respect to the total phytoplankton count sizes > 55 μm. This percentage increased further in the coastal area adjacent to Cape Baba. The total number of individuals increased logarithmically to (> 10^6 cells/l) near the coast at Cape Baba, and decreased gradually towards the east. In the same region, there was a parallel increase in the observed number of species close to the coast (54 coastal species *versus* ≈ 10 offshore species; the species richness index increased from a value of 1.2 in the offshore region to about 3.8 near the coast); but the corresponding measures of diversity decreased abruptly within the coastal band of cold water (Shannon-Wiener index < 0.1, evenness index = 0.02) as compared to the offshore regions (Shannon-Wiener index > 1.0, evenness index > 0.5).

Species density along the eastern Anatolian coast remained very low, albeit with relatively higher levels near Yesilirmak River, where the intense burst of the neritic species *Skeletonema costatum* yielded the lowest equitability measures (J' = 0.08). Species richness (d) in this part was also smaller, due to lower levels in abundance and number of species.

Two-dimensional non-metric MDS plots of gridded surface stations had six distinct groups at an arbitrary similarity level of 50 %. It is clearly shown that plankton sampled from the colder water drifted with the boundary current from the northwest shelf are placed within the larger most productive group (VI), which is distinguished from the others by higher abundance and species richness. Grid #7, together with the most easterly grids #18, #19, #20, and #21 constitute another group (II), with relatively warmer offshore waters coexisting in both sectors. It is apparent that the dominating species *Chaetoceros* sp. played a significant role in distinction between patches formed along the Turkish Black Sea coast, and that there is a strong biological response to mesoscale activity of the cold coastal current.

Acknowledgments

This work forms part of a Ph.D. thesis carried out within the framework of the project "Stock Assessment Studies for the Turkish Black Sea Coast" supported by the NATO "Science for Stability" Programme and the State Planning Organization (SPO); and is partially funded by the Turkish Scientific and Technical Research Council (TÜBİTAK). Sincere thanks are due to Professors Mustafa Ünsal and Ferit Bingel for their valuable suggestions in various ways. Generous help from Mr. Erhan Mutlu with the statistics is warmly acknowledged.

REFERENCES

Anon. (1992). Report of the FAO/IOC/UNEP Training Workshop on the Statistical Treatment and Interpretation of Marine Community Data. In cooperation with IOC/UNEP. Athens, February 1992, 212 p.

Baltic Sea Environment Proceedings (1988). Guideliness for the Baltic Monitoring Programme for the Third Stage.- 27 Part D., Biological Determinands. 161 p.

Benli H.A. (1987). Investigation of plankton distribution in the southern Black Sea and its effect on particle flux. In: *Particle Flux in the Ocean*. Ed. by E. T. Degens, E. Izdar, S. Honjo. Mitt. Geol.-Palaont. Inst. Univ. Hamburg. **62**, 77-87.

Bologa A.S. (1986). Planktonic primary productivity of the Black Sea: a review.- *Thalassia Jugoslavica* **21/22**, 1/2, 1-22.

Bologa A.S., H.V. Skolka, P.T. Frangopol (1984). Annual cycle of planktonic primary productivity off the Romanian Black Sea coast. *Mar. Ecol. Prog. Ser.* **19**, 25-32.

Hay B.J., S .Honjo (1989). Particle deposition in the present and holocene Black Sea. *Oceanography* **2**, 26-31.

Hay B.J., S. Honjo, S. Kempe, V.A. Itekkott, E.T. Degens, T. Konuk, E. Izdar (1990). Interannual Variability in Particle Flux in the Southwestern Black Sea. *Deep-Sea Res.* **37**, 911-928.

Hay B.J., M.A. Arthur, W.E. Dean, E.D. Neff (1991). Sediment Deposition in the Late Holocene Abyssal Black Sea: Terrigenous and Biogenic Matter. *Deep-Sea Res.* **38** (Suppl.), S711-S723.

Koblentz-Mishke O.J., V.V. Volkovinsky, J.G. Kabanova (1970). Plankton Primary Production of the World Ocean, p.183-193. In: *Scientific Exploration of the South Pacific*, W.S. Wooster, ed. National Academy of Sciences, Washington.

Malone T.C. (1980). Algal size in the physiological ecology of phytoplankton. – In: *The physiological ecology of phytoplankton*. Ed. by I. Morris. Blackwell Sci. Publ. Oxford. **7**, 433-463.

Oğuz T., V.S. Latun, M.A. Latif, V.V. Vladimirov, H.İ. Sur, A.A. Markov, E. Özsoy, B.B. Kotovshchikov, V.V. Eremeev, Ü. Ünlüata (1993). Circulation in the Surface and Intermediate Layers of the Black Sea, *Deep-Sea Res.* **40**, No.8, 1597-1612.

Oğuz T., D.G. Aubrey, V.S. Latun, E. Demirov, L. Koveshnikov, H.İ. Sur, V. Diaconu, S. Beşiktepe, M. Duman, R. Limeburner, V. Eremeev (1994). Mesoscale Circulation and Thermohaline Structure of the Black Sea Observed During HydroBlack '91. *Deep Sea Res.* **41**, 4, 603-628.

Özsoy E., Ü. Ünlüata, Z. Top (1993). The Mediterranean Water Evolution, Material Transport by Double Diffusive Intrusions and Interior Mixing in the Black Sea, *Progress in Oceanography.*

Sorokin Yu. I. (1983). The Black Sea. In: *Estuaries and Enclosed Seas, Ecosystems of the World*, B.H. Ketchum, editor, Elsevier, 253-292.

Stanev E.V. (1990). On the Mechanisms of the Black Sea Circulation, *Earth-Science Reviews* **28**, 285-319.

Sukhanova I.N., M.V. Flint, G. Hibaum, V. Karamfilov, A.I. Kopylov, E. Matveeva, T.N. Rat'kova, A.P. Sazhin (1988) *Exuviaella cordata* red tide in Bulgarian Coastal Waters (May to June 1986), *Marine Biology* **99**, 1-8.

Sur H.İ., E. Özsoy, Ü. Ünlüata (1994). Boundary current instabilities, upwelling, shelf mixing and eutrophication processes in the Black Sea. *Progress in Oceanography* **33**, 249-302.

Uysal Z. (1993). A preliminary study on some plankters along the Turkish Black Sea coast – species composition and spatial distribution –. Ph. D. Thesis. METU - Institute of Marine Sciences. Erdemli - Turkey. 138 p.

Venrick E.L. (1978). How many cells to count ? In: *Phytoplankton Manual*, A. Sournia, ed. UNESCO, U.K., 167-180.